Modeling for the Active Site of Sulfite Oxidase: Synthesis, Characterization, and Reactivity of $[Mo^{VI}O_2(mnt)_2]^{2-}$ (mnt^{2-} = 1,2-Dicyanoethylenedithiolate)

Samar K. Das, Pradeep K. Chaudhury, Dulali Biswas, and Sabyasachi Sarkar*

Contribution from the Department of Chemistry, Indian Institute of Technology, Kanpur, Kanpur-208016, India

Received January 4, 1994®

Abstract: The complexes, $[Bu_4N]_2[Mo^{VI}O_2(mnt)_2]$ (**1**), $[Bu_4N]_2[Mo^{IV}O(mnt)_2]$ (**2**), and $[Ph_3PNPPh_3][Et_4N][Mo^{V}OCl(mnt)_2]$ (**3**) (mnt^{2-} = 1,2-dicyanoethylenedithiolate) have been synthesized as possible models for active sites of sulfite oxidase which is proposed to contain molybdenum cofactor with dithiolene coordination around molybdenum. The structure of the $[Bu_4P]^+$ salt of complex anion of **1** has been determined by X-ray crystallography. The compound crystallizes in space group $P2_1/c$, with a = 14.200(3) Å, b = 19.402(4) Å, c = 18.967(3) Å, β = 95.48(1)°, and Z = 4. $[Mo^{VI}O_2(mnt)_2]^{2-}$ is a distorted octahedron with the oxo groups *cis* to each other and *trans* to the dithiolene sulfur atoms. The complexes **1–3** have been characterized by IR, UV–visible, ^{13}C NMR, and negative ion FAB mass spectra. Complex **1** shows a quasireversible reduction and proton coupled electron transfer reaction. Complex **2** undergoes an one-electron reversible oxidation; but on the coulometric time scale it disproportionates to a tris dithiolene complex, $[Mo^{IV}(mnt)_3]^{2-}$ and MoO_3. Complex **2** in the presence of Cl^- is oxidized irreversibly with the appearance of a new quasireversible couple corresponding to the electrochemical detection of $[Mo^{V}OCl(mnt)_2]^{2-}/[Mo^{IV}OCl(mnt)_2]^{3-}$. The EPR parameters of **3** and $[Mo^{V}O(mnt)_2]^{1-}$ are reported. The $^{35,37}Cl$ superhyperfine splitting of the chloro complex **3** is shown in relevance to Mo–Cl interaction in native sulfite oxidase. Complex **1** oxidizes HSO_3^- to HSO_4^- with the formation of **2** and without forming the biologically irrelevant μ-oxo Mo(V) dimer. This reaction follows enzymatic substrate saturation kinetics with apparent K_M (Michaelis–Menten constant) = 0.010(±0.001) M and k_2 (k_{Obs} at substrate saturation concentration and is proportional to V_{max}) = 0.87(±0.04) s^{-1} in MeCN/H_2O (1:1) medium at 20 °C.

Introduction

The enzyme, hepatic sulfite oxidase, is responsible for the physiologically important oxidation of sulfite to sulfate.[1] This enzyme is dimeric with each monomer containing a single Mo cofactor and a cyt b_5-type heme.[2] The conversion of sulfite or bisulfite to sulfate, a two-electron process, is presumed to occur at a Mo(VI) center, with the elements of water being used as the source of the additional oxygen atom of sulfate and the Mo(VI) is reduced to Mo(IV) state in the process 1.[2]

$$\text{enz–Mo}^{VI} + SO_3^{2-} + H_2O \rightarrow \text{enz–Mo}^{IV} + SO_4^{2-} + 2H^+ \quad (1)$$

To complete the catalytic cycle, the Mo(IV) is stepwisely reoxidized to Mo(VI) via Mo(V) by *b*-type heme of the enzyme, which is in turn reoxidized by the physiological electron acceptor *ferricytochrome c*.[3] All the three oxidation states of the molybdenum of sulfite oxidase have been studied by EXAFS[3] and EPR[4] techniques. The combined information is consistent with the following representations A, B, and C for the fully oxidized Mo(VI) state, intermediate Mo(V) state, and fully reduced Mo(IV) state respectively.

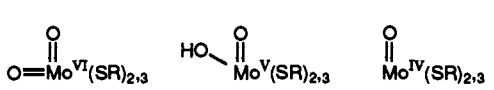

A B C

The two terminal oxo ligands of the Mo(VI) species are expected to be *cis* to one another with an O–Mo–O angle near 106°.[5a] One terminal oxo group appears to be present in the Mo(V) and Mo(IV) states[4a,b] of the enzyme. The hydroxo ligand of the Mo(V) species is suggested to be *cis* to the terminal oxo group as shown by ^1H superhyperfine splitting.[4] No oxomolybdoenzyme has yet been characterized by an X-ray crystal structure determination. However, Rajagopalan and co-workers have proposed a structure for the molybdenum cofactor from various spectroscopic measurements. The proposed structure for the molybdenum cofactor (representation D) depicts it as a complex of molybdopterin and Mo, with the metal linked to the dithiolene sulfurs.[5b] The

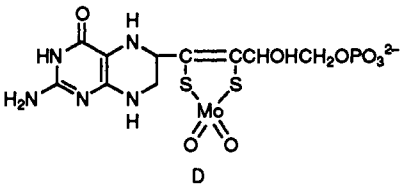

D

resonance Raman spectra of native dimethyl sulfoxide reductase, which also contains a molybdenum cofactor similar to that of sulfite oxidase, have been found to contain resonances attributable to molybdenum dithiolene.[6] The presence of a dithiolene linkage and pterin moiety at the active site of this enzyme may be important for its enzymatic action.

* Abstract published in *Advance ACS Abstracts*, September 1, 1994.

(1) (a) Kessler, D. L.; Rajagopalan, K. V. *J. Biol. Chem.* **1972**, *247*, 6566. (b) Bray, R. C. *Adv. Enzymol. Relat. Areas Mol. Biol.* **1980**, *51*, 107. (c) Bray, R. C. *Q. Rev. Biophys.* **1988**, *21*, 299.

(2) Rajagopalan, K. V. In *Molybdenum and Molybdenum Containing Enzymes*; Coughlan, M., Ed.; Pergamon Press: Oxford, 1980.

(3) George, G. N.; Kipke, C. A.; Prince, R. C.; Sunde, R. A.; Enemark, J. H.; Cramer, S. P. *Biochemistry* **1989**, *28*, 5075.

(4) (a) Cramer, S. P.; Gray, H. B.; Rajagopalan, K. V. *J. Am. Chem. Soc.* **1979**, *101*, 2772. (b) Cramer, S. P.; Wahl, R.; Rajagopalan, K. V. *J. Am. Chem. Soc.* **1981**, *103*, 7721. (c) Kessler, D. L.; Rajagopalan, K. V. *Biochim. Biophys. Acta* **1974**, *370*, 389. (d) Kessler, D. L.; Johnson, J. L.; Cohen, H. J.; Rajagopalan, K. V. *Biochim. Biophys. Acta* **1974**, *334*, 86.

(5) (a) Stiefel, E. I. In *Comprehensive Coordination Chemistry*; Wilkinson, G., Gillard, R. D., McCleverty, J. A., Eds.; Pergamon Press: New York, 1987; p 1375 (b) Kramer, S. P.; Johnson, J. L.; Ribeiro, A. A.; Millington, D. S.; Rajagopalan, K. V. *J. Biol. Chem.* **1987**, *262*, 16357.

(6) Gruber, S.; Kilpatrick, L.; Bastian, N. R.; Rajagopalan, K. V.; Spiro, T. G. *J. Am. Chem. Soc.* **1990**, *112*, 8179.

0002-7863/94/1516-9061$04.50/0

To understand the structure–function relationship of this class of enzymes containing the molybdenum cofactor, the following criteria[7] should be fulfilled by a model compound: (a) the mononuclear oxomolybdenum complex should have a linkage preferably with one dithiolene coordination, (b) the model complex should be capable of executing oxo transfer reactions with biologically relevant substrates, (c) it should not form the biologically irrelevant μ-oxo Mo(V) dimer during the course of the reaction, and (d) the oxidized Mo(VI) complex and reduced Mo(IV) complex should be interconvertible in both directions.

The preparations of molybdenum 1,2-enedithiolate complexes that contain C(6) pterins but do not contain a terminal oxo group, have recently been reported.[8] Numerous complexes containing the *cis*-dioxoMo(VI) unit and two or more sulfur donor ligands have been prepared.[9] The reactivity of these complexes has been tested, and they have been found to react with tertiary phosphines. A brief report by Spence[10] indicates that the complex $[MoO_2(o\text{-}C_6H_4(S)NHCH_2)_2]$ reacts with sulfite, but the reaction products have not been characterized. The catalytic aerobic oxidation of aldehydes to acids in the presence of the complex $[MoO_2(Cys\text{-}OEt)_2]$ (Cys-OEt = ethyl (*S*)-cysteinate) has been reported,[11] but the role of molybdenum is not described. For the reductase type of enzyme of this class, Holm and co-workers successfully used $MoO(LNS_2)$ [LNS_2 = 2,6-bis(2,2-diphenyl-2-mercaptoethyl)pyridine(2-)] to demonstrate functional analogue reactions for DMSO reductase, d-biotin d-(s-oxide) reductase, and nitrate reductase.[9a,12] Very recently Holm and his group have reported a molybdenum-mediated oxygen atom transfer reaction using the complex $MoO(t\text{BuL-NS})_2$ [*t*BuL-NS = bis(4-*tert*-butylphenyl)-2-pyridylmethanethiolate(1–)].[13] This complex is capable of executing an oxo transfer reaction with the biological substrate trimethylamine *N*-oxide. The molybdenum-(IV) dithiolene monooxo complex $[Et_4N]_2[Mo^{IV}O(bdt)_2]$ (bdt^{2-} = benzene-1,2-dithiolate) has also been shown to demonstrate analogue reaction for trimethylamine *N*-oxide reductase.[14a] However, for the oxidase-type enzymatic reaction 1, no model compound has yet been reported which effectively reacts with a physiological substrate like sulfite (bisulfite) or xanthine. The molybdenum-(VI) dithiolene dioxo complex $[Et_4N]_2[Mo^{VI}O_2(bdt)_2]$ has been reported,[14b] but its reactivity in oxo transfer reaction toward these substrates has not been reported. So the synthesis, characterization, redox chemistry, and reactivity toward biological substrates of such dithiolene complexes are of considerable interest with respect to modeling the proposed dithiolene coordination of molybdenum in the molybdenum cofactor.

As a part of our work in exploring dithiolate ligated oxomolybdenum complexes we have accomplished the synthesis of $[Bu_4N]_2[Mo^{VI}O_2(mnt)_2]$ (**1**), (mnt^{2-} = maleonitriledithiolate = 1,2-dicyanoethylenedithiolate). We report here the full description of synthesis, characterization, and electrochemistry of **1**, $[Bu_4N]_2[Mo^{IV}O(mnt)_2]$ (**2**), and $[Ph_3PNPPh_3][Et_4N][Mo^{V}OCl(mnt)_2]$ (**3**). The reduced product **2** synthesized by different procedures is known.[15,16] The functional analogue reaction of sulfite oxidase using complex **1** is also described in this paper. A preliminary report of some of these results has already appeared.[17]

Experimental Section

Materials. [*n*Bu_4N]Br, [*n*Bu_4P]Br, [Et_4N]Br, [Ph_3PNPPh_3]Cl, PPh_3, and [Bu_4N]Cl were obtained from Aldrich; $NaHSO_3$, from Merck; NaCN, from May and Baker Ltd.; $Na_2MoO_4\cdot 2H_2O$, from John Baker Inc.; molybdic acid, from Thomas Baker and Co. The chemicals were used as purchased. Solvents were distilled and dried by standard methods. Doubly distilled water was used to make the buffer solution.

Physical Measurements. Elemental analyses were determined with a EA 1108 elemental analyzer. Infrared spectra were recorded as CsI pellet on Perkin-Elmer 577 and FT 1600 series IR spectrophotometers. Electronic spectra were measured in different solvents by a Shimadzu 160 spectrophotometer. Negative ion FAB mass (FAB^-) spectra were recorded on a JEOL SX 102 DA-6000 mass spectrometer data system using argon (6 kV, 10 mA) as the FAB gas. The accelerating voltage was 10 kV, and the spectra were recorded at room temperature. *m*-Nitrobenzyl alcohol (3-NBA) was used as the matrix. ^{13}C NMR (100 MHz) spectra were obtained on a Bruker WM-400 FT NMR spectrometer using DMSO-d_6. Tetramethylsilane was used as an internal standard. Conductance measurements were performed at room temperature in MeCN solutions with an Elico CM-82T (Hyderabad, India) conductivity bridge. EPR spectra were obtained with a Varian E-109 spectrometer. Samples were prepared under N_2, transferred to EPR tubes with gas-tight syringes, and frozen immediately in liquid N_2. Room temperature solution spectra were obtained with a flat cell. EPR parameters were obtained from the measured spectra using DPPH as calibrant. Cyclic voltammetric measurements were made with CV 27 BAS Bioanalytical Systems and PAR model 370–4 Electrochemistry System. Cyclic voltammograms of 10^{-3} M solutions of the compounds were recorded either with glassy carbon or platinum working electrode in MeCN/0.1 M Et_4NClO_4 or in CH_2Cl_2/0.1 M Bu_4NClO_4. The experiments employed a Ag/AgCl or SCE reference electrode and platinum auxiliary electrode. Controlled potential electrolysis experiments were performed with a PAR Model 370–4 Electrochemistry System using a platinum wire gauze working electrode. All electrochemical experiments were done under dinitrogen atmosphere at 298 K. The solid state magnetic moment of the molybdenum(V) complex was measured with a Cahn Faraday balance, using $Hg[Co(NCS)_4]$ as calibrant; corrections for diamagnetic effects were made using Pascal's constants. X-ray powder diffraction patterns were measured using a Rich Seifert Isodebyeflex 2002 diffractometer.

Synthesis. 1,2-Dicyanoethylenedithiolate Disodium Salt or Maleonitriledithiolate Disodium Salt (Na_2mnt). This ligand was prepared by the procedure published by Stiefel *et al.*[16]

$[Bu_4N]_2[Mo^{VI}O_2(mnt)_2]$ (1). $Na_2MoO_4\cdot 2H_2O$ (0.485 g, 2.0 mmol) and Na_2mnt (0.745 g, 4.0 mmol) were taken in 40 mL of citric acid–phosphate buffer (pH ~6) at 10 °C. Bu_4NBr (5.0 mmol, ~1.6 g) was added whereupon a red brown oily mass formed. The oily mass solidified at room temperature. The red brown solid was crushed with a glass rod and washed, first with cold water and then with 2-propanol and diethyl ether. This product was crystallized from MeCN–2-propanol–diethyl ether: yield 1.1 g (61%); mp 100–103 °C dec; IR (CsI pellet, cm^{-1}) νMo=O, 890 (vs), 855 (s), νMo—S, 320 (s), ν(C=C), 1471 (vs); UV–vis (MeCN solution, 1×10^{-4} M, nm) 525, 425, 365; ^{13}C NMR (ppm from TMS) in DMSO-d_6, δ = 123.2, 117.5 (mnt), δ = 57.8, 23.21, 19.30, 13.52 (cation, n-Bu_4N); FAB^- in 3-nitrobenzyl alcohol, 410 = P^-, 394 = $P^- - [O]$, 652 = $P^- + Bu_4N^+$; conductivity (MeCN, 10^{-3} M solution at 298 K) Λ_M = 247 mho cm^2 mol^{-1} consistent with a 2:1 electrolyte. Anal. Calcd for $C_{40}H_{72}MoN_6O_2S_4$: C, 53.78; H, 8.12; N, 9.40; S, 14.35. Found: C, 53.99; H, 7.87; N, 9.66; S, 14.66.

The $[Bu_4P]^+$ salt was prepared and isolated in the same way as the $[Bu_4N]^+$ salt: IR (CsI pellet, cm^{-1}) νMo=O, 885 (vs), 850 (s), νMo—S, 318 (s), ν(C=C), 1479; UV–vis (MeCN solution, 1×10^{-4} M, nm) 525, 425, 365. Anal. Calcd for $C_{40}H_{72}MoN_4O_2P_2S_4$: C, 51.81; H, 7.82; N, 6.04; S, 13.83. Found: C, 51.94; H, 7.71; N, 5.98; S, 13.94.

(7) Holm, R. H.; Berg, J. M. *Acc. Chem. Res.* **1986**, *19*, 363.
(8) Pilato, R. S.; Eriksen, K. A.; Greaney, M. A.; Stiefel, E. I.; Goswami, S.; Kilpatrick, L.; Spiro, T. G.; Taylor, E. C.; Rheingold, A. L. *J. Am. Chem. Soc.* **1991**, *113*, 9372.
(9) (a) Holm, R. H.; Berg, J. M. *J. Am. Chem. Soc.* **1985**, *107*, 917, 925. (b) Kaul, B. B.; Enemark, J. H.; Merbs, S. L.; Spence, J. T. *J. Am. Chem. Soc.* **1985**, *107*, 2885. (c) Reynolds, M. S.; Berg, J. M.; Holm, R. H. *Inorg. Chem.* **1984**, *23*, 3057. (d) Palanca, P.; Picher, T.; Sanz, V.; Gomez-Romero, P.; Llopis, E.; Domenech, A.; Cervilla, A. *J. Chem. Soc., Chem. Commun.* **1990**, 531. (e) Holm, R. H. *Chem. Rev.* **1987**, *87*, 1401. (f) Moore, F. W.; Larson, M. L. *Inorg. Chem.* **1967**, *6*, 998. (g) Roberts, S. A.; Young, C. G.; Cleland, W. E., Jr.; Ortega, R. B.; Enemark, J. H. *Inorg. Chem.* **1988**, *27*, 3044.
(10) Spence, J. T.; Minelli, M.; Kroneck, P. *J. Am. Chem. Soc.* **1980**, *102*, 4538.
(11) Speier, G. *Inorg. Chim. Acta* **1979**, *33*, 139.
(12) Craig, J. A.; Holm, R. H. *J. Am. Chem. Soc.* **1989**, *111*, 2111.
(13) Schultz, B. E.; Gheller, S. F.; Muetterties, M. C.; Scott, M. J.; Holm, R. H. *J. Am. Chem. Soc.* **1993**, *115*, 2714.
(14) (a) Oku, H.; Ueyama, N.; Kondo, M.; Nakamura, A. *Inorg. Chem.* **1994**, *33*, 209. (b) Yoshinaga, N.; Ueyama, N.; Okamura, T.; Nakamura, A. *Chem. Lett.* **1990**, 1655.
(15) McCleverty, J. A.; Locke, J.; Ratchiff, B.; Wharton, E. J. *Inorg. Chim. Acta* **1969**, *3*, 283.
(16) Stiefel, E. I.; Bennett, L. E.; Dori, Z.; Crawford, T. H.; Simo, C.; Gray, H. B. *Inorg. Chem.* **1970**, *9*, 281.
(17) Sarkar, S.; Das, S. K. *Proc. Indian Acad. Sci. (Chem. Sci.)* **1992**, *104*, 437.

$[Bu_4N]_2[Mo^{IV}O(mnt)_2]$ (2). This compound was reported earlier.[15,16] Three alternative synthetic methods are as follows:

Method 1. Molybdic acid ($H_2MoO_4 + H_2O$) (0.36 g, 2.0 mmol) and Na_2mnt (0.745 g, 4.0 mmol) were taken in ~100 mL of water. The reaction mixture was slightly heated until undissolved molybdic acid reacted and went into solution. $NaHSO_3$ (0.21 g, 2.0 mmol) was then added and the yellow red solution changed to green brown. Addition of Bu_4NBr (1.6 g, 5.0 mmol) caused precipitation of a dirty green solid, which was collected by filtration and washed, first with water and then with 2-propanol and diethyl ether. This green product was crystallized from a mixture of MeCN, 2-propanol, and diethyl ether: yield 1.17 g (66%), mp 148–151 °C; IR (CsI pellet, cm^{-1}) νMo=O, 928 (vs), νMo—S, 335 (s), ν(C=C), 1482 (vs); UV–vis (MeCN solution, 1×10^{-4} M, nm) 602, 491, 395 (sh), 363; ^{13}C NMR (ppm from TMS) in DMSO-d_6, δ = 130.52, 118.90 (mnt), 57.56, 22.98, 19.07, 13.26 (cation, nBu_4N); FAB$^-$ in 3-nitrobenzyl alcohol, 394 = P^-, 636 = P^- + Bu_4N^+; conductivity (MeCN, 10^{-3} M solution at 298 K) Λ_M = 280 mho cm^2 mol^{-1} consistent with a 2:1 electrolyte. Anal. Calcd for $C_{40}H_{72}MoN_6OS_4$: C, 54.76; H, 8.27; N, 9.58; S, 14.62. Found: C, 54.88; H, 8.12; N, 9.66; S, 14.77.

The $[Et_4N]^+$ salt was obtained in the same way as the $[Bu_4N]^+$ salt. Anal. Calcd for $C_{24}H_{40}MoN_6OS_4$: C, 44.15; H, 6.17; N, 12.87; S, 19.64. Found: C, 44.03; H, 6.26; N, 13.04; S, 19.59. Conductivity (MeCN, 10^{-3} M solution at 298 K) Λ_M = 274 mho cm^2 mol^{-1} is consistent with a 2:1 electrolyte.

The $[Bu_4P]^+$ salt was also obtained. Anal. Calcd for $C_{40}H_{72}MoN_4OP_2S_4$: C, 52.73; H, 7.96; N, 6.15; S, 14.07. Found: C, 52.88; H, 8.01; N, 6.09; S, 14.13.

Method 2. A solution of 0.58 g (0.648 mmol) of **1** in 6 mL of MeCN was treated with a solution of 0.17 g (1.61 mmol) of $NaHSO_3$ in 4 mL of water resulting immediately in a green oily mass. This oily mass solidified within 6 h. The solid was filtered and washed with 2-propanol and diethyl ether. The product was crystallized from a mixture of MeCN, 2-propanol, and diethyl ether. The yield of **2** was 0.524 g (92%).

Method 3. A solution of 0.050 g (0.191 mmol) of Ph_3P in 4 mL of MeCN was added to a solution of 0.096 g (0.107 mmol) of **1** in 6 mL of MeCN. This was stirred for 2 h when the deep red solution was changed to a dirty green color. Addition of 2-propanol and excess diethyl ether caused a green solid **2** to crystallize. This solid was recrystallized from MeCN–2-propanol–diethyl ether. The yield of **2** in this process was 0.075 g (80%).

Estimation of Sulfate Formed in the Reaction between 1 and $NaHSO_3$. All solvents used in this process were deaerated by argon purging before use. In a typical experiment a solution of 0.58 g (0.648 mmol) of **1** in 6 mL of MeCN was treated with a solution of 0.17 g (1.61 mmol) of $NaHSO_3$ in 4 mL of water resulting immediately in a green oily mass. After 15 min, 25 mL of water was added into it and filtered. The gummy mass was washed with another 15 mL of water in portions. To the filtrate combined with the washings was added dropwise an aqueous 0.1 M solution of $BaCl_2$ to complete the precipitation of a white solid. The precipitate was allowed to settle for about 8 h. This was filtered off through a weighted filtering crucible (G-4) and washed repeatedly with 0.5 M hydrochloric acid until the washings showed negative sulfite reaction (the dissolved $BaSO_3$ in dilute hydrochloric acid precipitates $BaSO_4$ on oxidation with bromine water). The precipitate was finally washed with water and estimated gravimetrically for $BaSO_4$. The blank experiment was performed by taking 0.17 g (1.61 mmol) of $NaHSO_3$ without using **1**. Subsequent steps were followed identically and the time involved before filtering off the precipitate was kept the same as was done before. Repeated washings of this precipitate with 0.5 M hydrochloric acid dissolved most of the precipitated $BaSO_3$ leaving a small quantity of insoluble $BaSO_4$ which was gravimetrically estimated. The weight of the precipitate (0.016 g) obtained by the blank experiment was subtracted from the previous weight (0.164 g) to get the correct amount of $BaSO_4$ (0.148 g) formed by the reaction between **1** and $NaHSO_3$. The conversion was 98 ± 0.3% on the basis of three determinations. The identity of the precipitated $BaSO_4$ was confirmed by comparing its X-ray powder diffractogram with that of authentic $BaSO_4$.

$(PyH)_2[Mo^{IV}O(mnt)_2]$. Molybdic acid (0.36 g, 2.0 mmol) and of Na_2-mnt (0.745 g, 4.0 mmol) were taken in 15 mL of water. The reaction mixture was heated to get a clear yellow red solution. $NaHSO_3$ (0.21 g, 2.0 mmol) was added when the color of the solution changed to greenish brown. The solution was then filtered. Addition of 0.5 mL of acetic acid and 0.8 mL of pyridine to it caused the precipitation of a crystalline solid, $(PyH)_2[Mo^{IV}O(mnt)_2]$. This was recrystallized from MeCN–2-propanol–diethyl ether: yield 0.75 g (58%); IR (CsI pellet, cm^{-1}) νMo=O, 906 (vs), νMo—S, 332 (s), νC=C, 1485 (vs); UV–vis (MeCN solution, 1×10^{-4} M, nm) 602, 491, 395 (sh), 363. Anal. Calcd for $C_{18}H_{12}MoN_6OS_4$: C, 39.13; H, 2.19; N, 15.21; S, 23.21. Found: C, 39.21; H, 2.30; N, 15.18; S, 23.31.

Table 1. Summary of X-ray Diffraction Data for $[Bu_4P]_2[Mo^{VI}O_2(mnt)_2]$

chemical formula	$C_{40}H_{72}MoN_4O_2P_2S_4$
fw	927.19
space group	$P2_1/c$
a, Å	14.200(3)
b, Å	19.402(4)
c, Å	18.967(3)
β, deg	95.48(1)
V, Å^3	5220(4)
Z	4
d_{calc}, g cm^{-3}	1.18
μ, cm^{-1}	5.1
T, °C	25°
scan type	$\theta - 2\theta$
R	0.060
R_w	0.064

Attempted Synthesis of $[Mo^VO(mnt)_2]^{1-}$. Synthesis of $[Et_4N]_2[Mo^{IV}(mnt)_3]$. Iodine (0.13 g, 1.02 mmol) in 5 mL of CH_2Cl_2 was added with stirring to a green brown solution of $[Et_4N]_2[Mo^{IV}O(mnt)_2]$ (0.652 g, 1.0 mmol) in 15 mL of CH_2Cl_2. The color of the solution immediately turned green. Stirring was continued for 2 h. 2-Propanol (20 mL) was added when a kelly green solid separated. This was collected by filtration, washed with 2-propanol and diethyl ether, and was crystallized from a mixture of MeCN, 2-propanol, and diethyl ether, giving needle-shaped crystals: yield 0.388 g (50%). Anal. Calcd for $C_{28}H_{40}MoN_8S_6$: C, 43.28; H, 5.18; N, 14.42; S, 24.75. Found: C, 43.30; H, 5.23, N, 14.40; S, 24.79. The electronic spectrum of this complex matched exactly with that of the reproted[16,18] $[Bu_4N]_2[Mo^{IV}(mnt)_3]$.

$[Ph_3PNPPh_3][Et_4N][Mo^VOCl(mnt)_2]$ (3). Iodine (0.13 g, 1.02 mmol) in 5 mL of CH_2Cl_2 was added with stirring to a solution of 0.652 g (1.0 mmol) $[Et_4N]_2[Mo^{IV}O(mnt)_2]$ in 15 mL of CH_2Cl_2 containing excess $[Ph_3PNPPh_3]Cl$. Stirring was continued for another half hour. MeOH (10 mL) and an excess of petroleum ether were added to precipitate a sea green solid. This microcrystalline product was washed with petroleum ether and dried in vacuo at room temperature: yield 0.877 g (80%); IR (CsI pellet, cm^{-1}) νMo=O, 933 (s), νMo—S, 330 (m), νC=C, 1483 (s); UV–vis (CH_2Cl_2 solution in the presence of excess Cl^-, 1×10^{-4} M, nm) 650, 491, 336; solid state magnetic moment, μ_{eff} = 1.86 μ_B (at room temperature). Anal. Calcd for $C_{52}H_{50}MoN_6OClP_2S_4$: C, 56.96; H, 4.59; N, 7.66; S, 11.69. Found: C, 56.98; H, 4.63; N, 7.72; S, 11.75.

X-ray Structural Determination of $[Bu_4P]_2[Mo^{VI}O_2(mnt)_2]$. Summary of X-ray diffraction data for $[Bu_4P]_2[Mo^{VI}O_2(mnt)_2]$ is given in Table 1. Air stable crystals of the $[Bu_4P]^+$ salt of **1** were obtained as red rectangular shape on keeping its solution in MeCN–2-propanol–diethyl ether at 0 °C for 2 days. The compound crystallizes in monoclinic space group $P2_1/c$. Lattice parameters were obtained by least-squares analysis of 25 machine-centered reflections with $20° \le 2\theta \le 30°$. The intensities of three standard reflections were monitored periodically (every 97 reflections) throughout the course of data collection; no significant decay was detected. The structure was solved by the direct method and refined on F by full-matrix least-squares techniques. The XTAL3.2 package[19] and a PC-486 computer were used for all calculations. Difficulties were encountered in locating all the carbon atoms of each $[Bu_4P]^+$ cation. Both the cations were disordered showing high temperature factors. All H atom positions were calculated but they are not included in the structure factor calculations as they did not show any noticeable effect on the R values. After the final stage of refinement, the largest peak in the difference Fourier map had a height of 0.81e^-/Å^3 and was located near the C(40) of Bu_4P^+. The final atomic positional and thermal parameters for $[Bu_4P]_2[Mo^{VI}O_2(mnt)_2]$ have been deposited as supplementary material.

Kinetic Measurements on Oxidation of $NaHSO_3$ by 1. All kinetic measurements were made by a spectrophotometric method by use of Shimadzu 160 spectrophotometer provided with a piezoelectric-type thermostating device for the regulation of temperature. Since $NaHSO_3$ is soluble in aqueous medium while the complex **1** is soluble in organic

(18) McCleverty, J. A.; Locke, J.; Wharton, E. J. *J. Chem. Soc. (A)* **1968**, 816.

(19) *XTAL3.2 Reference Manual*; Hall, S. R., Flack, H. D., Stewart, J. M., Eds.; University of Western Australia: Geneva and Maryland, 1992.

medium, the advantage of mixed solvent medium (1:1) MeCN:H_2O was taken. All experiments were performed with argon flushed deaerated solvents. The fixed wave length, 535 nm, was chosen to monitor the progress of the reaction, since at this wave length the difference in the optical density between **1** and **2** is at a maximum. As the half-life of this reaction was almost of the order of few seconds at higher concentrations of $NaHSO_3$, a modification of conventional procedure was adopted for the kinetic measurements.[20] The concentration of the stock solution of complex **1** in MeCN and separate stock solutions of $NaHSO_3$ in MeCN:H_2O (12:13, v/v) of different strength were prepared so as to have a desired fixed concentration of the complex **1** (4.098×10^{-4} M) in the reaction mixture while the concentration of $NaHSO_3$ in the same mixture could be varied. $NaHSO_3$ solution (2.9 mL) was placed in the spectrophotometer cell with the help of a calibrated pipette and left for a minute or so to acquire the desired temperature. A total of 100 μL of the complex **1** in MeCN was placed with the help of a micropipet (Sigma) on the flat button of glass attached to one end of a glass rod of five inches length. This was lowered into the cell and the solutions were mixed with a few vertical rapid movements of the rod. As soon as the button was dipped into the solution already contained in the cell, a stopwatch was started. The progress of the reaction was monitored by the decay of absorbance as a function of time. Three kinetic runs were made for each $NaHSO_3$ concentration over the entire range of $NaHSO_3$ concentration used. The substrate concentration was varied ranging from 50×10^{-4}M to 250×10^{-4}M. The rate law was found to be always first order in complex **1** over this substrate concentration range as found using conventional graphical procedure. The decay of the complex **1** in terms of concentration follows eq 2

$$C_t = (A_t - A_\infty)/(\epsilon_1 - \epsilon_2) \quad (2)$$

where C_t is the molar concentration of the complex **1** at time t, A_t and A_∞ are the absorbances of the reaction mixture solution at time t and at time $t = \infty$ respectively, ϵ_1 (1580 M^{-1} cm^{-1}) and ϵ_2 (82 M^{-1} cm^{-1}) are the molar extinction coefficients of the complex **1** and **2**, respectively, at 535 nm in 1:1 MeCN:H_2O mixed medium. The temperature at which substrate ($NaHSO_3$) saturation kinetics was performed was 20 ± 0.1 °C.

Results and Discussion

Synthesis. The synthetic aspect of $[Mo^{VI}O_2(mnt)_2]^{2-}$ has a special relevance in relation to its model behavior. The starting precursor is sodium molybdate. The tetrahedral $[MoO_4]^{2-}$ anion is readily soluble in water in common pH ranges. The stabilization of the MoO_2^{2+} core using mnt^{2-} ligand in aqueous medium is difficult because of the pH dependent hydrolytic equilibria[21] of molybdate anion and the easy oxidation of mnt^{2-} ligand.[22] For MoO_4^{2-}, as the pH is lowered from 7, protonation followed by expansion of the coordination number from 4 to 6 occurs.[21] This process results in the formation of MoO_2^{2+} core which may readily complex with mnt^{2-} to produce the desired complex. However, the simultaneous formation of polyoxomolybdate anions at lower pH will deplete the concentration of MoO_2^{2+}. Furthermore, polyoxomolybdates, like heptamolybdate around pH < 6, are potent oxidizing agents of mnt^{2-}. To overcome the formation of heptamolybdate anion, we have carried out the reaction in phosphate buffer (pH 6.0–6.6). The reaction forming the desired complex must remain in equilibrium with other reactions involving oxomolybdenum(VI) species. Addition of counter cation (Bu_4N^+/Bu_4P^+) preferentially drives the reaction in the desired way by phasing out the complex salt from the reaction medium. The role of the phosphate buffer is important in this synthesis. The binding of phosphate ion to the $Mo^{VI}O_2$ entity of the molybdenum cofactor of sulfite oxidase in buffer solution has recently been reported.[23] In this synthesis phosphate ion seems to stabilize the MoO_2^{2+} core in buffer solution. The importance of the phosphate buffer can be judged by the reaction between

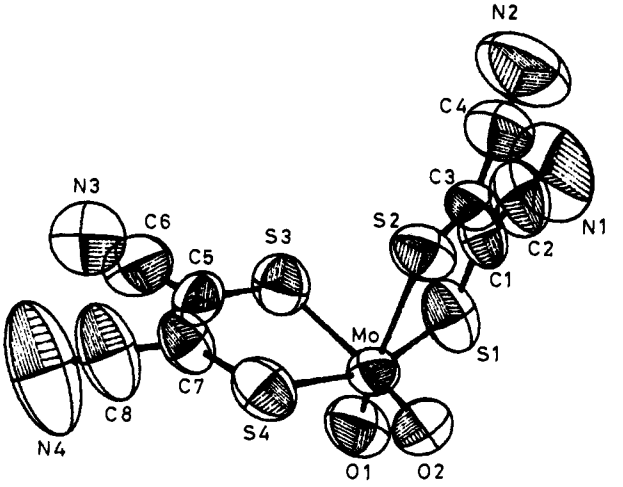

Figure 1. Structure and labeling of the $[Mo^{VI}O_2(mnt)_2]^{2-}$ anion in $[Bu_4P]_2[Mo^{VI}O_2(mnt)_2]$. Thermal ellipsoids as drawn by ORTEP represent the 50% probability surfaces.

molybdic acid and Na_2mnt in aqueous solution. In this case, even MoO_3 is capable of oxidizing the ligand resulting in the reduction of Mo(VI) to Mo(IV) and the reduced species, $[Mo^{IV}O(mnt)_2]^{2-}$, can be precipitated out by a counter cation. The low yield (30%) of this reduced product is due to the absence of sufficient free mnt^{2-}. This is substantiated by the fact that when this reaction was carried out in the presence of bisulfite ($NaHSO_3$), the yield of the desired reduced product is over 60%. The reduced monooxo complex, $(PyH)_2[Mo^{IV}O(mnt)_2]$, was isolated when molybdic acid, Na_2mnt, and $NaHSO_3$ were taken in water containing pyridine and CH_3COOH. This pyridinium salt is soluble in phosphate buffer (pH ~7.5).

The well-known molybdenum complexes containing $Mo^{VI}O_2S_4$ and $Mo^{IV}OS_4$ moiety of dithiocarbamate series are the best studied compounds of molybdenum in relevance to oxomolybdoenzymes. For this series of complexes it is the comproportionation[9e] reaction 3 which complicates most of its redox reactions parallel to

$$Mo(VI) + Mo(IV) \rightarrow Mo_2(V) \quad (3)$$

enzymatic oxo transfer reactions. However, in oxomolybdoenzymes, the molybdenum cofactor is surrounded by bulky apoprotein which imposes steric crowding and thus prevents dimerization. When the complexes **1** and **2** were mixed together in MeCN, they did not undergo the biologically irrelevant comproportionation reaction 4 to yield the μ-oxomolybdenum(V) dimer; upon workup

$$[Mo^{VI}O_2(mnt)_2]^{2-} + [Mo^{IV}O(mnt)_2]^{2-} \not\rightarrow [(mnt)_2Mo^{V}(O)\text{–}O\text{–}(O)Mo^{V}(mnt)_2]^{4-} \quad (4)$$

only starting complexes **1** and **2** were recovered.

The complex **2** can be oxidized chemically by iodine or electrochemically in a one-electron step in CH_2Cl_2 to $[Mo^{V}O(mnt)_2]^{1-}$ (checked by EPR spectrum), but this Mo(V) species as a monoanion could not be isolated; instead, upon workup, the tris dithiolene complex $[Bu_4N]_2[Mo^{IV}(mnt)_3]$ was obtained from the reaction mixture. This may be due to disproportionation of $[Mo^{V}O(mnt)_2]^{1-}$ to $[Mo^{IV}(mnt)_3]^{2-}$ and MoO_3 (*vide infra*). However, when the complex, $[Et_4N]_2[Mo^{IV}O(mnt)_2]$ was oxidized by an equivalent amount of iodine in CH_2Cl_2 in presence of excess of $[Ph_3PNPPh_3]Cl$ the Mo(V) species was isolated as $[Ph_3PNPPh_3][Et_4N][Mo^{V}OCl(mnt)_2]$.

Description of Structure of $[Bu_4P]_2[Mo^{VI}O_2(mnt)_2]$. The unit cell of this compound contains discrete mononuclear molecules of $[Bu_4P]_2[Mo^{VI}O_2(mnt)_2]$. The structure of the anion, $[Mo^{VI}O_2(mnt)_2]^{2-}$, is presented in Figure 1 and selected bond

(20) Below, J. F.; Connick, R. E.; Coppel, C. P. *J. Am. Chem. Soc.* **1958**, *80*, 2961.
(21) Stiefel, E. I. *Prog. Inorg. Chem.* **1977**, *22*, 34.
(22) Simmons, H. E.; Blomstrom, D. C.; Vest, D. R. *J. Am. Chem. Soc.* **1962**, *84*, 4756.
(23) Spence, J. T.; Kipke, C. A.; Enemark, J. H.; Sunde, R. A. *Inorg. Chem.* **1991**, *30*, 3011.

Table 2. Selected Bond Distances (Å) and Angles (Deg) in $[Mo^{VI}O_2(mnt)_2]^{2-}$

	Bond Distances		
Mo–O1	1.69(1)	C1–C3	1.24(5)
Mo–O2	1.73(1)	C5–C7	1.38(3)
Mo–S1	2.411(6)	C1–S1	1.55(3)
Mo–S2	2.563(6)	C3–S2	1.82(4)
Mo–S3	2.607(5)	C5–S3	1.73(2)
Mo–S4	2.428(6)	C7–S4	1.64(2)
	Bond Angles		
O1–Mo–O2	101.5(6)	Mo–S1–C1	110.5(9)
O2–Mo–S1	106.4(4)	Mo–S4–C7	111.2(8)
O1–Mo–S4	112.1(4)	Mo–S3–C5	102.9(8)
S1–Mo–S2	80.1(2)	S2–Mo–S3	85.3(2)
S3–Mo–S4	79.3(2)	S1–Mo–S4	159.7(2)

distances and angles are listed in Table 2. The structure of the complex anion is a distorted octahedron with the oxo groups *cis* to each other and *trans* to sulfur atoms. The sulfur atoms *trans* to the oxo groups must compete with the strongly bound oxo groups for the same orbital.[24] This *trans* effect is reflected in the Mo–S2 (2.563(6) Å) and Mo–S3 (2.607(5) Å) distances compared to Mo–S1 (2.411(6) Å) and Mo–S4 (2.428(6) Å) distances (Table 2) which are not *trans* to terminal oxo groups. The Mo–O and Mo–S bond distances are important because these are the only evaluated structural parameters from EXAFS analysis of enzymatic molybdenum site. The values of 1.69(1) Å (Mo–O1 distance) and 1.73(1) Å (Mo–O2 distance) fall close to the range of 1.66–1.72 Å (for Mo–O distance) in enzymatic molybdenum sites.[4b,25] Similarly, the values of 2.411(6) Å (Mo–S1 distance) and 2.428(6) Å (Mo–S4 distance) fall within the range 2.41–2.47 Å for Mo–S distances in molybdoenzymes. The ligand has the expected geometry. Bond lengths and angles within the mnt^{2-} ligand of $[Mo^{VI}O_2(mnt)_2]^{2-}$ are consistent with the values found for the complex anion $[Mo^{IV}(mnt)_3]^{2-}$.[26] The structure of $MoO_2(Et_2dtc)_2$ is also a distorted octahedron with the oxo groups *cis* to each other and *trans* to sulfur atoms.[27] The X-ray structure of MoO_2(dttd) (dttdH_2 = 2,3:8,9-dibenzo-1,4,7,-10-tetrathiadecane) indicates that the molecule adopts a distorted octahedral geometry with the thioether atoms *trans* to the terminal oxo groups which are *cis* to each other.[9b] Therefore, the structure of $[Mo^{VI}O_2(mnt)_2]^{2-}$ anion is consistent with other dioxomolybdenum(VI) complexes with similar donor atoms.

Spectroscopy. IR. The complex **1** exhibits two strong ν(Mo=O) bands at 855 and 890 cm^{-1} characteristic of the *cis*-$[MoO_2]^{2+}$ fragment. The presence of two Mo–O_t bands in the IR spectra of virtually all six-coordinate MoO_2^{2+} compounds is strongly indicative of the *cis*-dioxo structure.[28] The frequencies for the stretching vibrations of $[MoO_2]^{2+}$ core in complex **1** are considerably lower. This lowering indicates that the better π donor ligands, mnt^{2-}, located *cis* to the two terminal oxo ligands can compete for the available vacant dπ (mainly d_{xz} and d_{yz}) orbitals of the metal atom, thereby reducing the bond order between the metal atom and the terminal oxygen atoms. Complex **1** shows a strong (IR) band at 320 cm^{-1} which is assigned to Mo–S vibration, and the reduced complex **2** has a strong Mo–S band at 335 cm^{-1}. That the νMo–S is slightly lower for the Mo(VI) in **1** than for the Mo(IV) in **2** is in agreement with the enzyme dimethyl sulfoxide reductase.[6] This trend reflects stronger ligation of dithiolene to Mo(IV) than to Mo(VI) in molybdenum cofactor of sulfite oxidase.[29]

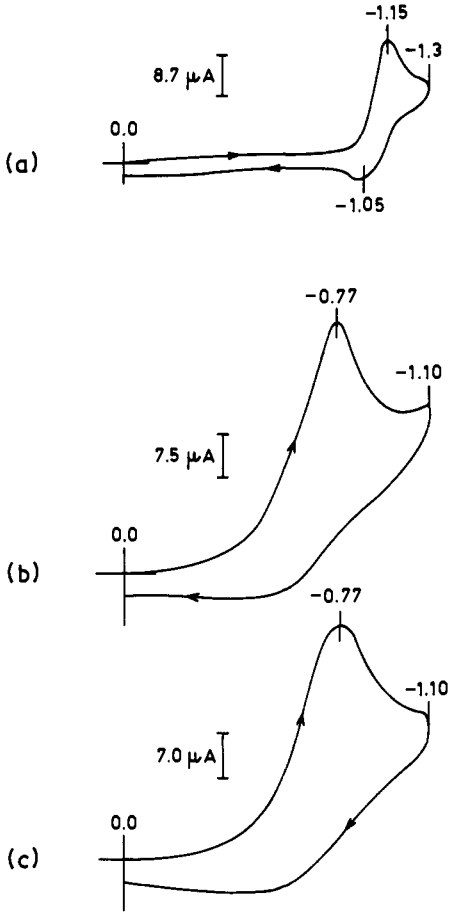

Figure 2. Cyclic voltammograms of $[Bu_4N]_2[Mo^{VI}O_2(mnt)_2]$: (a) in MeCN, (b) in MeCN with 0.13 M CH_3COOH and 3.5 M H_2O, (c) in MeCN with 0.13 M CH_3COOD and 3.5 M D_2O (1×10^{-3} M samples; 0.10 M Et_4NClO_4; scan rate = 0.100 V s^{-1}; peak potentials *vs* Ag/AgCl).

UV–Visible. The electronic spectrum of **1** consists of three bands with λ_{max} (ϵ_M) = 525 (1620), 425 (6866), and 365 (6244) nm. The absorption spectrum of the dioxomolybdenum(VI) complex having four donor atoms, MoO_2(dttd)[9b] showed a λ_{max} at 410 nm and a weaker band at ~480 nm.[30] The similarity of the donor atoms of Mo in complexes **1** and in MoO_2(dttd) and the knowledge of the resonance Raman spectra[30] of the latter complex suggest the broad absorption at 525 nm of complex **1** is dithiolene $S^- \rightarrow$ Mo(VI) charge transfer type of transition. The band at 425 nm is assigned to O $\rightarrow$ Mo(VI) transition. The high-energy band at 365 nm could be due to dithiolene intraligand transition. The absorption spectrum of the oxidized Mo fragment of rat liver sulfite oxidase has λ_{max} at ~480 and 350 nm.[31] The broad band at ~480 nm thus may be due to dithiolene S $\rightarrow$ Mo(VI) charge transfer transition.

Electrochemistry. The cyclic voltammograms (CV) of complex **1** in MeCN in the presence of Et_4NClO_4 exhibits a quasireversible reduction centered at –1.1 V *vs* Ag/AgCl with ΔE_p = 100 mV (Figure 2a). The $i_{pc} > i_{pa}$ suggests the instability of the reduced species even under CV time scale. Coulometric reduction of **1** in MeCN at –1.3 V gave a yellow red solution after addition of 2.28 electrons per molecule after a period of a half hour (when Coulomb count was still increasing). The electronic spectrum of this yellow red solution showed the presence of free dithiolate ligand, indicating decomposition of the compound. A similar decomposed product has been obtained by the coulometric reduction of neutral compound, $MoO_2(LNS_2)$ (LNS_2, *vide supra*)

(24) Cotton, F. A. In *Proceedings of the First International Conference on the Chemistry and Uses of Molybdenum*; Climax Molybdenum Company: London, 1973; p 6.
(25) Cramer, S. P.; Solomonson, L. P.; Adams, M. W. W.; Mortenson, L. E. *J. Am. Chem. Soc.* **1984**, *106*, 1467.
(26) Brown, G. F.; Stiefel, E. I. *Inorg. Chem.* **1973**, *12*, 2140.
(27) Berg, J. M.; Hodgson, K. O. *Inorg. Chem.* **1980**, *19*, 2180.
(28) Stiefel, E. I. In *Molybdenum and Molybdenum Containing Enzymes*; Coughlan, M., Ed.; Pergamon Press: Oxford, 1980; p 41.
(29) Rajagopalan, K. V.; Johnson, J. L. *J. Biol. Chem.* **1992**, *267*, 10199.
(30) Subramanian, P.; Burgmayer, S.; Richards, S.; Szalai, V.; Spiro, T. G. *Inorg. Chem.* **1990**, *29*, 3849.
(31) (a) Johnson, J. L.; Rajagopalan, K. V. *J. Biol. Chem.* **1977**, *252*, 2017. (b) Rajagopalan, K. V. In ref 2, p 241.

which showed a nearly reversible CV centered at –0.88 V *vs* SCE.[9a] A possible explanation for the decomposition of **1** within the coulometric time span is the instability of **1** in the presence of OH^- generated in the reduction of trace amount of H_2O present in the solvent. The electronic spectrum of the complex **1** in 1:1 MeCN/phosphate buffer in water (pH ~8) exhibited rapid decrease in the height of the peaks (525 and 425 nm) with the end feature identical to the absorption spectrum of free dithiolate ligand within a period of 5 min.

When the cyclic voltammogram of **1** was recorded in MeCN containing 0.13 M CH_3COOH and 3.5 M H_2O, the quasireversible reduction couple (at –1.1 V *vs* Ag/AgCl) became irreversible and the cathodic peak potential dropped to –0.77 V *vs* Ag/AgCl (Figure 2b). This change from quasireversible to irreversible reduction can be understood easily because the reduced species containing $MoO_2(V)$, being more basic in nature, gets protonated.[9a] The drop in reduction potential may be due to a proton coupled electron transfer reaction. Confirmation regarding the proton coupled electron transfer reaction has been borne out by recording the cyclic voltammogram of **1** in MeCN containing 0.13 M CH_3COOD and 3.5 M D_2O (Figure 2c). The isotopic kinetic effect with the change of proton to deuterium can be understood by observing the profile of reduction peaks in these two cases as shown in Figure 2, parts b and c. The broad nature of the cathodic peak of the deuterated system compared to that of the protonated system confirmed the participation of proton coupled electron transfer in this electrochemical reduction.[32] Controlled potential coulometry of **1** in MeCN containing 0.13 M CH_3COOH and 3.5 M H_2O at –1.0 V was performed. The value of n (n = number of electrons) was found to be 2.5 after a half hour (when Coulomb count was still increasing). After coulometry the solution was EPR silent and its electronic spectrum showed the presence of $[Mo^{IV}O(mnt)_2]^{2-}$ along with some free dithiolate ligand. The coulometric time scale as well as the applied potential at –1.0 V in the acidic medium may be responsible for the decomposition of the complex resulting in the formation of free dithiolate ligand with the increase of number of Coulomb count beyond 2.

The tetravalent complex anion of **2**, $[Mo^{IV}O(mnt)_2]^{2-}$, undergoes a reversible one-electron oxidation (with ΔE_p = 70 mV) in MeCN in the presence of Et_4NClO_4 at +0.445V *vs* Ag/AgCl (Figure 3a). However, on the coulometric time scale, the complex anion, $[Mo^{IV}O(mnt)_2]^{2-}$, is converted to the tris dithiolene complex, $[Mo^{IV}(mnt)_3]^{2-}$. Coulometric oxidation of **2** at +0.70 V after the removal of ~1 electron/molecule gave a bright green EPR silent solution. The CV of this bright green solution exhibits a new quasireversible oxidation at +0.70 V *vs* Ag/AgCl and a new reversible reduction process centered at –1.12 V *vs* Ag/AgCl. This CV is identical with the CV obtained from the authentic Mo(IV) tris dithiolene complex, $[Et_4N]_2[Mo^{IV}(mnt)_3]$.[16,18] The electronic spectrum of this bright green solution is also the same as that of tris dithiolene complex in MeCN. These results indicate that the initial one-electron oxidized Mo(V) product, $[Mo^{V}O(mnt)_2]^{1-}$, which is very unstable in MeCN, rapidly changes to the tris dithiolene Mo(IV) complex, $[Mo^{IV}(mnt)_3]^{2-}$, by a disproportionation reaction under the influence of trace amount of water present in the solvent. These results are interpreted in Scheme 1.

The reaction sequence in Scheme 1 can be explained by EC (electron transfer followed by chemical transformation) mechanism. The pyridinium salt, $(PyH)_2[Mo^{IV}O(mnt)_2]$, exhibits an irreversible reduction at –1.30 V *vs* Ag/AgCl in addition to the usual reversible oxidation centered at +0.45 V *vs* Ag/AgCl (Figure 3b). This reduction peak is assigned to the reduction of pyridine.

The electrochemical behavior of complex **2** in CH_2Cl_2 in the presence of Bu_4NClO_4 includes a chemically reversible one

(32) Manchanda, R.; Thorp, H. H.; Brudvig, G. W.; Crabtree, R. H. *Inorg. Chem.* **1991**, *30*, 494.

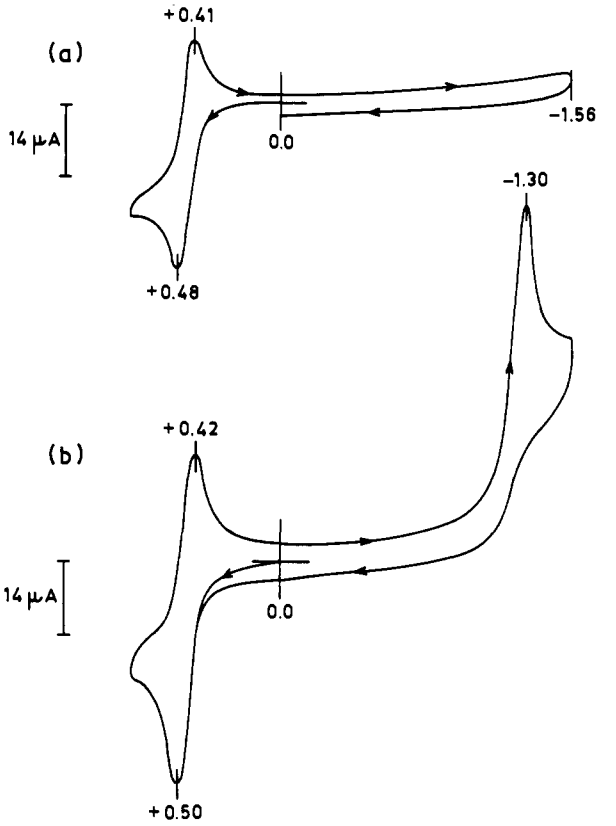

Figure 3. Cyclic voltammograms of (a) $[Bu_4N]_2[Mo^{IV}O(mnt)_2]$ and (b) $(pyH)_2[Mo^{IV}O(mnt)_2]$ in MeCN (1×10^{-3} M samples; 0.10 M Et_4NClO_4; scan rate = 0.100 V s^{-1}; peak potentials *vs* Ag/AgCl).

Scheme 1

$$[Bu_4N]_2[Mo^{IV}O(mnt)_2] - e^- \overset{+0.445\,V}{\rightleftharpoons} [Bu_4N][Mo^{V}O(mnt)_2] + [Bu_4N]^+$$

$$3[Bu_4N][Mo^{V}O(mnt)_2] + [Bu_4N]^+ + H_2O \xrightarrow{\text{disproportionation}} 2[Bu_4N]_2[Mo^{IV}(mnt)_3] + H_2MoO_4$$

electron oxidation (i_{pa}/i_{pc} = 0.92) at +0.44 V *vs* SCE (Figure 4a). Coulometric oxidation of **2** at +0.70 V removes 0.9 electron/molecule after a period of a half hour and gives an EPR active solution. The EPR spectrum (g = 1.991) which corresponds to the species, $[Mo^{V}O(mnt)_2]^{1-}$ is shown in Figure 6a The same EPR spectrum was obtained chemically by the oxidation of **2** in CH_2Cl_2 by iodine (*vide infra*). After coulometry the CV was almost unchanged but an additional small height couple (marked at Figure 4b) was observed at ~0.61 V. The authentic tris dithiolene complex, $[Mo^{IV}(mnt)_3]^{2-}$ also exhibited a reversible couple in CH_2Cl_2 around +0.61 V *vs* SCE. Thus after coulometry the solution contains mainly the Mo(V) species, $[Mo^{V}O(mnt)_2]^{1-}$ with some amount of $[Mo^{IV}(mnt)_3]^{2-}$. After 1 h this solution did not give any EPR spectrum and the electronic spectrum of this was almost identical to the spectrum of the authentic tris dithiolene complex, $[Et_4N]_2[Mo^{IV}(mnt)_3]$ in CH_2Cl_2. These results suggest that the initial one-electron oxidized species, $[Mo^{V}O(mnt)_2]^{1-}$, disproportionates ultimately to $[Mo^{IV}(mnt)_3]^{2-}$ but at a slow rate in CH_2Cl_2 and at a faster rate in MeCN (Scheme 1).

When the cyclic voltammetry of **2** was performed in the presence of Cl^- ($[Ph_3PNPPh_3]Cl$ or Ph_4PCl) in CH_2Cl_2, the reversible oxidation process (Figure 4a) became irreversible (Figure 4c); when the scan rate was increased to 500 mV/s, another quasireversible couple centered at –0.20 V *vs* SCE appeared along with the irreversible one (Figure 4c). This indicates that Cl^- binds to molybdenum center in this oxidation process. These observations are consistent with Scheme 2. The binding of Cl^- to molybdenum(V) has been confirmed by EPR spectroscopy

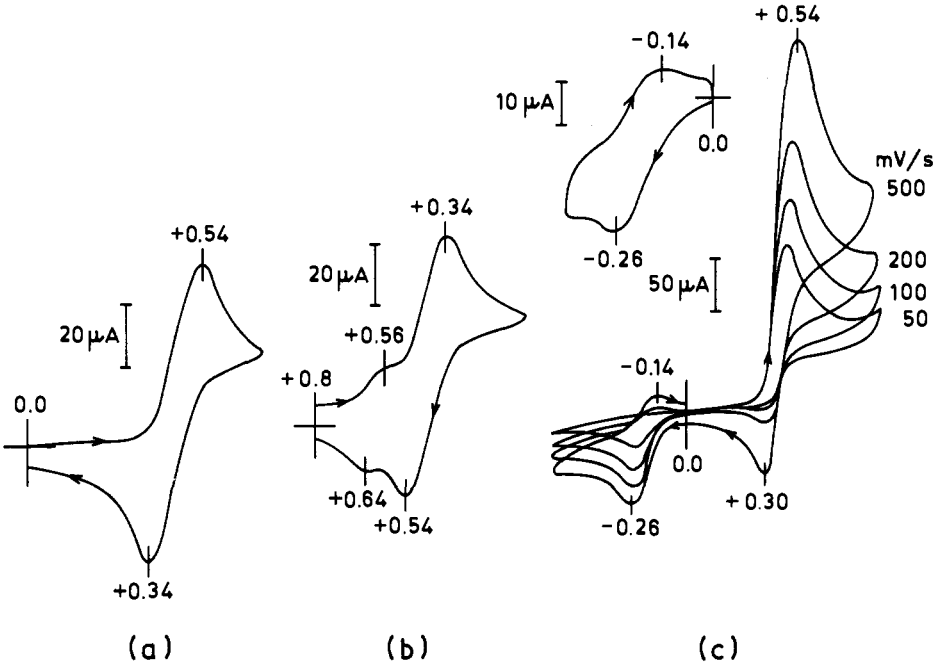

Figure 4. (a) Cyclic voltammogram of $[Bu_4N]_2[Mo^{IV}O(mnt)_2]$ in CH_2Cl_2, (b) cyclic voltammogram after Coulometry of $[Bu_4N]_2[Mo^{IV}O(mnt)_2]$ in CH_2Cl_2 (resting potential at + 0.8 V), and (c) cyclic voltammograms of $[Bu_4N]_2[Mo^{IV}O(mnt)_2]$ in the presence of excess $[Ph_3PNPPh_3]Cl$ in CH_2Cl_2 at different scan rates as indicated (1×10^{-3} M samples; 0.1 M Bu_4NClO_4; peak potentials *vs* SCE).

Scheme 2

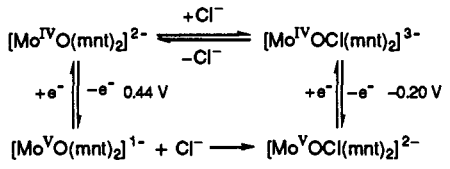

(*vide infra*). The chloro–Mo(V) complex, $Mo^{V}OCl(dttd)$, has been reported which exhibits a reduction process centered at –0.18 V *vs* SCE.[9b] The electrochemistry of $MoO(LNS_2)$ in DMF containing 0.1 M Et_4NCl developed a scheme where Cl^- is suggested to be bound to both $MoO(LNS_2)$ and $MoO(LNS_2)^{1+}$ in solution.[9a] These facts support Scheme 2. The reduction potentials of the molybdenum center of sulfite oxidase are strongly dependent on coordinating anions: chloride binds to both Mo(V) and Mo(IV) states of sulfite oxidase.[3,23] Therefore the molybdenum(V) species, $[MoOCl(mnt)_2]^{2-}$ (Scheme 2) may be related to the EPR active site of sulfite oxidase. The synthesis of this chloro–Mo(V) complex, $[Mo^{V}OCl(mnt)_2]^{2-}$ has been carried out by chemical means. When $[Et_4N]_2[Mo^{IV}O(mnt)_2]$ was oxidized by an equivalent amount of iodine in CH_2Cl_2 containing excess of $[Ph_3PNPPh_3]Cl$, the $Mo^{V}OCl$ species was isolated as $[Ph_3PNPPh_3][Et_4N][Mo^{V}OCl(mnt)_2]$ (**3**). The CV of this complex **3** showed the quasireversible redox couple at –0.20 V *vs* SCE (inset, Figure 4c) which was identical to that seen at –0.20 V *vs* SCE in cyclic voltammograms of **2** in CH_2Cl_2 at different scan rates in presence of $[Ph_3PNPPh_3]Cl$ (Figure 4c).

EPR. Since the molybdenum cofactor contains a dithiolene coordination around molybdenum, the effect of such coordination on the g and A ($^{95,97}Mo$) values is of considerable interest. The oxobis(benzene-1,2-dithiolato)molybdenum(V) complex, $[Ph_4P][Mo^{V}O(bdt)_2]$, (H_2bdt = benzene-1,2-dithiol), has been structurally established but with no EPR data;[33] The EPR data for the monodithiolene oxo Mo(V) complex LMoO(2-S,S) (L = hydrotris(3,5-dimethyl-1-pyrazolyl)borate, 2-S,S = toluene-3,4-dithiolate) are known[34] which are consistent with S_2N_3 coordination. When complex **3** was dissolved in CH_2Cl_2 and immediately subjected to EPR measurement, two molybdenum(V) signals having g values at 1.991 and 1.974, respectively, appeared as shown in Figure 5. With time the intensity of the signal with $g = 1.974$ decreased with the increase of the intensity of the signal with $g = 1.991$. When $[Ph_3PNPPh_3]Cl$ was added in excess into the test solution, the EPR signal with $g = 1.991$ completely vanished with the appearance of a signal with $g = 1.974$ (Figure 6b). When **2** was oxidized by 1 equiv of iodine in CH_2Cl_2 and subjected to room temperature EPR measurement only one signal with $g = 1.991$ ($[Mo^{V}O(mnt)_2]^{1-}$) was observed (Figure 6a). When excess $[Ph_3PNPPh_3]Cl$ was added the signal with $g = 1.991$ disappeared and the signal with $g = 1.974$ appeared (Figure 6b). These experiments clearly demonstrate the presence of the two molybdenum(V) species: one is in the five-coordinated form, $[Mo^{V}O(mnt)_2]^{1-}$ (g = 1.991) and another is in six-coordinated form with Cl^- coordination, $[Mo^{V}OCl(mnt)_2]^{2-}$ (g

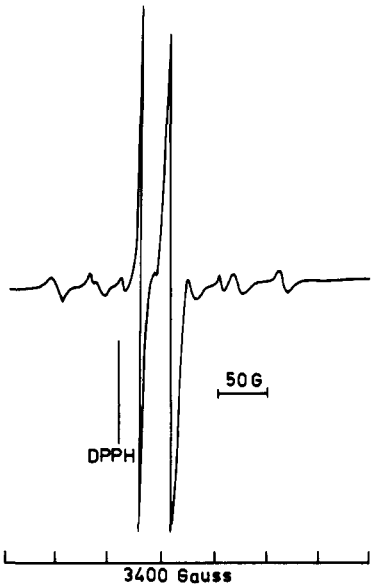

Figure 5. EPR spectrum of $[Ph_3PNPPh_3][Et_4N][Mo^{V}OCl(mnt)_2]$ (1×10^{-3} M in CH_2Cl_2 at room temperature).

(33) Boyde, S.; Ellis, S. R.; Garner, C. D.; Clegg, W. *J. Chem. Soc., Chem. Commun.* **1986**, 1541.
(34) Cleland, W. E., Jr.; Barnhart, K. M.; Yamanochi, K.; Collision, D.; Mabbs, F. E.; Ortega, R. B.; Enemark, J. H. *Inorg. Chem.* **1987**, *26*, 1017.

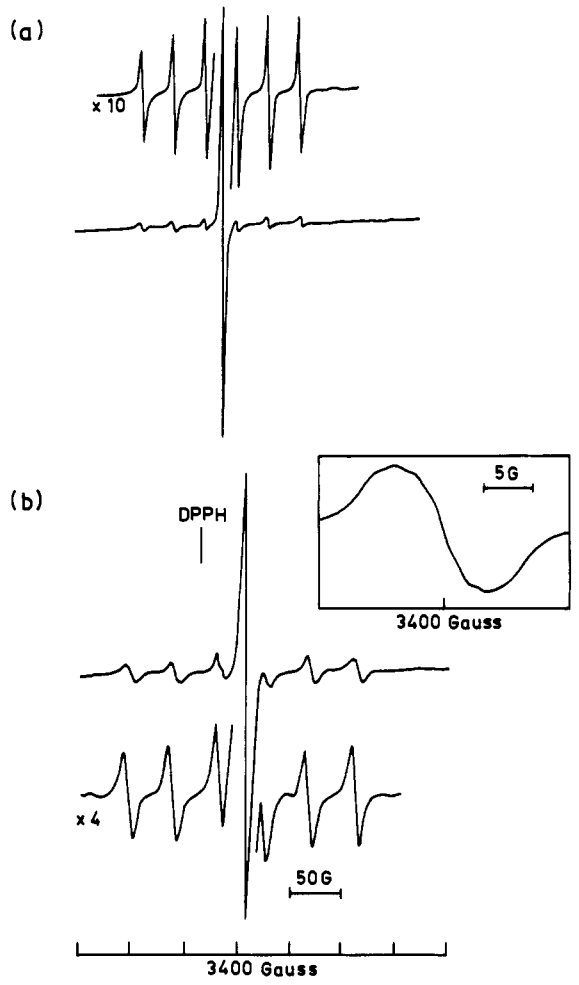

Figure 6. (a) EPR spectrum of $[Mo^{V}O(mnt)_2]^{1-}$ formed by chemical oxidation of $[Bu_4N]_2[Mo^{IV}O(mnt)_2]$ by an equivalent amount of iodine in CH_2Cl_2 at room temperature and (b) EPR spectrum of $[Ph_3PNPPh_3][Et_4N][Mo^{V}OCl(mnt)_2]$ in the presence of excess $[Ph_3PNPPh_3]$-Cl at room temperature; inset, the main signal of chloro compound in expanded form.

= 1.974), which are in equilibrium as shown in (eq 5).

$$[Mo^{V}OCl(mnt)_2]^{2-} \rightleftharpoons [Mo^{V}O(mnt)_2]^{1-} + Cl^- \quad (5)$$

Chloride has two isotopes of ^{35}Cl and ^{37}Cl and both have $I = {}^3/_2$ with combined neutral abundance 100%. $^{35,37}Cl$ superhyperfine splitting (four components) should be observed if the attachment of Cl^- is *cis* to Mo=O group because the unpaired electron in the molybdenum(V) complex is located in d_{xy} orbital.[35] If the attachment of Cl^- is *trans* to Mo=O group then no superhyperfine splitting due to Cl^- interaction should be observed. A careful search of the main signal (g = 1.974) in expanded form clearly showed superhyperfine splitting due to Cl^- interaction as shown in the inset of Figure 6b and by inspection the $A(^{35,37}Cl)$ value was estimated to be of 3.4 G. Similar interaction of Cl^- has been reported for the complex, $[MoOCl(S_2CNEt_2)_2]$ with $A(^{35,37}Cl)$ = 3.0 G.[36] The magnitude of the chlorine superhyperfine splitting is small because of its low nuclear magnetic moment value. It was thought that the corresponding bromo system having higher nuclear magnetic moment value would respond to this type of superhyperfine splitting with larger separation. However, addition of Ph_4PBr in excess into $[Mo^{V}O(mnt)_2]^{1-}$ generated by an equivalent amount of iodine

(35) Garner, C. D.; Bristow, S. In *Molybdenum Enzymes*; Spiro, T. G., Ed.; John Wiley: New York, 1985; p 343.
(36) Chen, G. J.-J.; McDonald, J. W.; Newton, W. E. *Inorg. Chim. Acta* **1980**, *41*, 49.

Table 3. EPR Parameters[a] for $[Mo^{V}O(mnt)_2]^{1-}$ (X) and $[Mo^{V}OCl(mnt)_2]^{2-}$ (Y)[b]

					^{95,97}Mo (mT)			
center	g_1	g_2	g_3	$\langle g\rangle_{rt}$	A_1	A_2	A_3	$\langle A\rangle_{rt}$
X	2.015	1.982	1.960	1.991	4.5	0.59	4.0	3.025
Y	1.998	1.963	1.950	1.974				4.35

[a] CH_2Cl_2; g values and $\langle A\rangle$, A_1, A_3 values obtained from spectra; A_2 calculated from $\langle g\rangle\langle A\rangle = {}^1/_3(g_1A_1 + g_2A_2 + g_3A_3)$. rt = room temperature, all other values at 77 K. [b] In the presence of excess $[Ph_3PNPPh_3]Cl$.

oxidation of $[Mo^{IV}O(mnt)_2]^{2-}$ did not affect the g value (=1.991) of $[Mo^{V}O(mnt)_2]^{1-}$, suggesting that Br^- did not bind to molybdenum(V) center. The ^{19}F superhyperfine coupling in the EPR spectrum of molybdenum(V) species of sulfite oxidase at low pH form indicates the presence of Mo–F ligation[3] which is presumed to be analogous to the Mo–Cl interaction found by the effect of Cl^- on the molybdenum(V) EPR signal of chicken liver sulfite oxidase.[3] The EPR spectrum of $[Mo^{V}O(mnt)_2]^{1-}$ species in CH_2Cl_2 (generated chemically by iodine or electrochemically) at 77 K is indicative of rhombic symmetry with high g values and low A values as expected for S_4 coordination (Table 3). The EPR spectrum of the Mo(V) complex, $[MoO(SCH_2CH_2S)_2]^{1-}$ at 77 K exhibited a rhombic signal with g = 1.995[37] but the anisotropic EPR spectrum of the thiolate complex, $[MoO(SPh)_4]^{1-}$ is axial with g = 1.990.[38] These observations suggest that the dithiolene sulfur donors are comparable to thiolate sulfur donor or ethane-1,2-dithiol donors in their effect on Mo(V) g values. The EPR spectrum of $[Mo^{V}OCl(mnt)_2]^{2-}$ in the presence of excess $[Ph_3PNPPh_3]Cl$ at 77 K exhibits a slight rhombic distortion from axial symmetry with g = 1.974 (Table 3). Therefore, addition of Cl^- to $[Mo^{V}O(mnt)_2]^{1-}$ changes the rhombic symmetry of this monoanion to almost axial symmetry with the formation of Cl^- bound dianion, $[Mo^{V}OCl(mnt)_2]^{2-}$. The reported complex, MoOCl(dttd), also has axial symmetry at 77 K with g = 1.974.[9b]

Functional Analogue Reactions of Sulfite Oxidase. Complex **1** was tested to see whether it reacted with the biological substrate sulfite (or bisulfite). Na_2SO_3 when dissolved in water raises the pH of the solution because of the following reaction:

$$Na_2SO_3 + H_2O \rightleftharpoons NaHSO_3 + NaOH \quad (6)$$

The complex is not stable in solution at pH greater than 7. Thus to avoid the hydrolysis and decomposition of **1** at higher pH, we have used $NaHSO_3$ as substrate. The stability of **1** in a solution containing acetic acid has been checked by following electronic spectrum of **1** in MeCN and after the addition of acetic acid. The spectrum does not change. This suggests that on acidification, the protonation of the oxo group in **1** does not take place and molybdenum–dithiolene ligation remains intact. This observation is in accord with the EXAFS results of the oxidized form of sulfite oxidase wherein it was shown that the dioxo form in the oxidized state does not protonate at low pH.[3] However it has been observed that if the pH is lowered below 4 the $[Mo^{VI}O_2(mnt)_2]^{2-}$ species is decomposed.

The spectrophotometric course of the reaction between **1** and $NaHSO_3$ in MeCN–H_2O (3.3% water) is presented in Figure 7. As the spectrum of the molybdenum(VI) complex **1**, with λ_{max} = 365, 425, and 525 nm, diminishes with time, a clean isosbestic point at 374 nm is observed, and the final spectrum with maxima at 363, 491, and 602 nm is identical with that of **2**. This figure clearly demonstrates quantitative reduction of **1** by HSO_3^- to **2** according to

(37) Ellis, S. R.; Collision, D.; Garner, C. D.; Clegg, W. *J. Chem. Soc., Chem. Commun.* **1986**, 1483.
(38) Hanson, R. G.; Brunette, A. A.; McDonnell, A. E.; Murray, K. S.; Wedd, A. G. *J. Am. Chem. Soc.* **1981**, *103*, 1953.

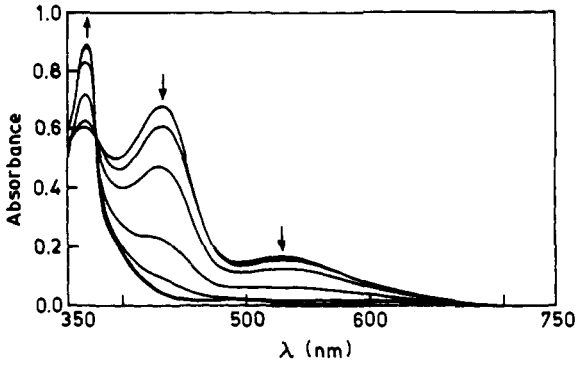

Figure 7. Spectral changes in the reaction of 1×10^{-4} M $[Bu_4N]_2[Mo^{VI}O_2(mnt)_2]$ and 1.5 equiv of $NaHSO_3$ in MeCN with 3.3% water at 25 °C.

$$[Mo^{VI}O_2(mnt)_2]^{2-} + HSO_3^- \xrightarrow{MeCN-H_2O} [Mo^{IV}O(mnt)_2]^{2-} + HSO_4^- \quad (7)$$

Quantification of the formation of sulfate in the above reaction was made gravimetrically by $BaSO_4$ method (*vide supra*).

The reaction is first order in Mo(VI) complex **1** as shown by the linearity of plots of log C_t *vs* time in experiments with greater than 12 equiv of $NaHSO_3$. The observed rate constants (k_{obs}) were obtained from the slopes of these plots. A plot of observed rate constants (k_{obs}) *vs* $[NaHSO_3]$ is shown in Figure 8a. At a sufficiently higher concentration of $NaHSO_3$ the k_{obs} becomes virtually independent of $[NaHSO_3]$. The plot of k_{obs} *vs* $[NaHSO_3]$ is indicative of a preequilibrium between **1** and $NaHSO_3$,[39a] as shown in Scheme 3. Scheme 3 is similar to the Michaelis–Menten scheme often encountered for the kinetics of enzyme catalyzed reactions,[39b] except that in this model case, **1** is not regenerated in the overall reaction. In any case, Scheme 3 leads to the formulation of the following expressions (see supplementary material):

$$k_{obs} = \frac{k_2[S]}{K_M + [S]} \quad (8)$$

where $K_M = (k_2 + k_{-1})/k_1$ or

$$\frac{1}{k_{obs}} = \frac{1}{k_2} + \frac{K_M}{k_2[S]} \quad (9)$$

For the special case in which $k_2 \ll k_{-1}$, K_M simplifies to k_{-1}/k_1; experimental results suggest that this is the case for the present system. Therefore a plot of $1/k_{obs}$ *vs* $1/[S]$ should give a straight line with $1/k_2$ as the y intercept and K_M/k_2 as the slope; again this plot is analogous to the Lineweaver–Burk plot obtained for a real enzyme. The $-x$ axis intercept equals $1/K_M$. The double reciprocol plot of $1/k_{obs}$ *vs* $1/[S]$ is shown in Figure 8b. k_2 and K_M were calculated from this plot as 0.87 (±0.04) s^{-1} and 0.010 (±0.001) M respectively at 20 °C.

The equilibrium formation of the intermediate complex (Scheme 3) $\{MoO_2(SO_3H)(mnt)_2\}^{3-}$ similar to enzyme–substrate (ES)[40] complex in enzymatic reaction is very important. In native sulfite oxidase, sulfite (or bisulfite) binds to the molybdenum center of the enzyme. In the present model study, binding of HSO_3^- to the molybdenum center is possible in two ways. First, the six-coordinated complex anion can bind to bisulfite with prior breaking of one of the Mo–S bonds (preferentially that *trans* to one of the oxo groups) and thus maintains 6-coordination in the formation of ES type complex. Alternatively, bisulfite can bind to molybdenum center with coordination expansion. However, seven-coordinated complexes containing the MoO_2(VI) moiety are not known. Thus to invoke seven-coordination for molybdenum(VI)–bisulfite complex, the so called ES complex, the initial MoO_2(VI) moiety in the complex should transform to MoO(VI) moiety to accommodate bisulfite ligation. Similar seven-coordinated MoO(VI) complexes are known.[41]

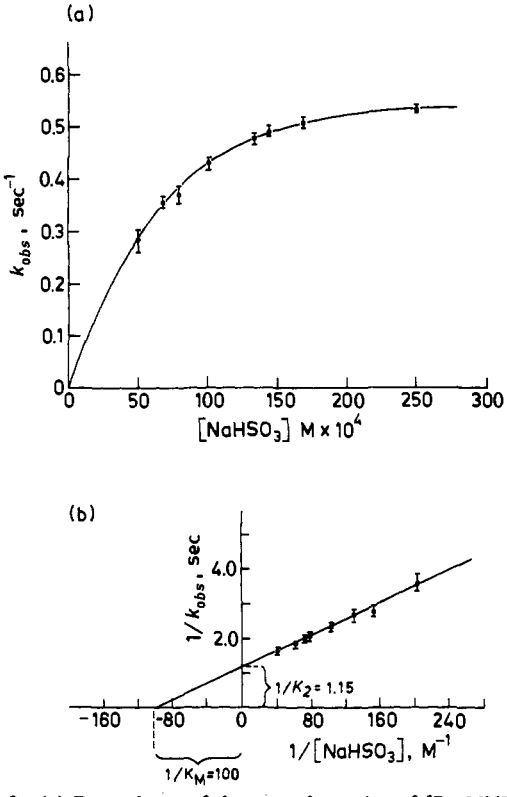

Figure 8. (a) Dependence of the rate of reaction of $[Bu_4N][Mo^{VI}O_2(mnt)_2]$ and 12–60 equiv of $NaHSO_3$ in MeCN–water (1:1) at 20 °C on $[NaHSO_3]$; (b) the corresponding double reciprocal plot.

Scheme 3

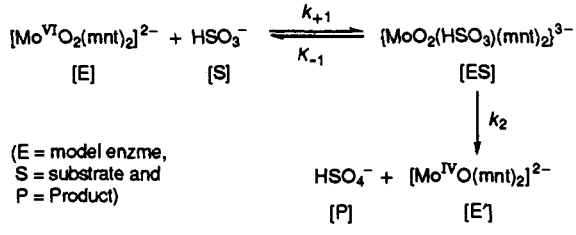

For demonstrating the back reaction, **2** to **1**, we decided to use $K_3[Fe(CN)_6]$ as this has been successfully used to oxidize the reduced molybdenum fraction of sulfite oxidase after tryptic cleavage.[31a] When the pyridinium salt of the reduced Mo(IV) complex, $(PyH)_2[MoO(mnt)_2]$, dissolved in phosphate–citric acid buffer (pH 7.5) was treated with 2 equiv of $K_3[Fe(CN)_6]$ the green solution changed immediately to red brown. Quick addition of Bu_4NBr in excess into the solution separated a red oily mass which on dissolving in a minimum amount of MeCN and adding 2-propanol ether precipitated analytically pure **1** in 10% yield only. This reaction thus confirmed the oxidation of reduced MoO(IV) species to the oxidized MoO_2(VI) species with the incorporation of the additional oxo group from water. The ferricyanide

(39) (a) Atkins, P. W. In *Physical Chemistry*, 4th ed.; W. H. Freeman and Co.: New York, 1990; p 802. (b) Lehninger, A. L. In *Principles of Biochemistry*; Worth Publishers: New York, 1982; p 207.

(40) The existence of a protic equilibrium mixture of the bound and of the free substrate species at the effective pH ~5.5 of the reaction mixture is a possibility.

(41) (a) Bradbury, J. R.; Schultz, F. A. *Inorg. Chem.* **1986**, *25*, 4416. (b) McDonald, J. W.; Newton, W. E. *Inorg. Chim. Acta* **1980**, *44*, L81. (c) Newton, W. E.; McDonald, J. W.; Corbin, J. L.; Ricard, L.; Weiss, R. *Inorg. Chem.* **1980**, *19*, 1997 and references cited therein.

oxidation is very fast and much of the compound is decomposed with the oxidation of the dithiolate ligand.[22] In native sulfite oxidase also, ferricyanide causes oxidative modification of the site with the loss of molybdenum.[4c]

Thus the most significant observation is made to demonstrate synthetic analogue reactions of sulfite oxidase using complexes **1** and **2**.

Conclusion: Comparison with the Active Site of Sulfite Oxidase

In the active site of sulfite oxidase, molybdenum(VI) is proposed to be ligated by two oxo groups and a dithiolate type of ligand.[5b] The complex **1** also contains *cis*-dioxo grouping and dithiolene coordination.

IR studies suggest that the dithiolate ligands are strongly bound to molybdenum(IV) (in complex **2**) and weakly bound to molybdenum(VI) (in complex **1**). In native enzyme also, the linkage of dithiolene in molybdenum(IV) is much stronger than molybdenum(VI).[29]

Cyclic voltammogram of **1** in MeCN showed quasireversible reduction at −1.1 V *vs* Ag/AgCl. But when this same CV was recorded in MeCN containing 0.13 M MeCOOH and 3.5 M H_2O, the quasireversible reduction couple at −1.1 V became irreversible and reduction peak potential shifted to less negative potential at −0.77 V *vs* Ag/AgCl which is due to a proton coupled electron transfer reaction. Nearly all the oxomolybdoenzymes process both hydrogens and electrons in one fashion or another.[42]

Interestingly, the electronic spectrum of **1** in MeCN was identical to that in MeCN containing 0.13 M MeCOOH and 3.5 M H_2O. This observation is in accord to the EXAFS results of the oxidized form of sulfite oxidase wherein it was shown that the dioxo form in the oxidized state does not protonate at low pH.[3]

The complex anion of **3**, $[Mo^{V}OCl(mnt)_2]^{2-}$, partially mimics the low pH form of the molybdenum(V) state of sulfite oxidase in the presence of excess of Cl^-. The EPR parameters for $[Mo^{V}OCl(mnt)_2]^{2-}$ are similar to those of sulfite oxidase (g = 1.980, A_1 = 6.3 mT at low pH form).[43]

Reduced Mo(IV) species have been oxidized back to MoO_2-(VI) species by ferricyanide with the incorporation of the additional oxo group from water.

Complex **1**, which contains biologically relevant coordination, reacts with the biological substrate, HSO_3^- in MeCN–water to produce HSO_4^- and reduced monooxo complex **2** quantitatively without forming the biologically irrelevant (μ-oxo)molybdenum-(V) dimer. Since sulfite (SO_3^{2-}) is in equilibrium with bisulfite (HSO_3^-) at physiological pH, it is not clear which is the actual substrate for the enzyme.[44] However, the close association of the activity of sulfite oxidase with mitochondrial electron sequence reaction and the low pH available in mitochondrial reaction strongly suggests the reactive substrate be preferably HSO_3^-.

Acknowledgment. We are grateful to Professor P. K. Bharadwaj for help in the X-ray structure analysis and to Professor R. N. Mukherjee for the use of PAR electrochemical equipments. Support of this work and of the National X-ray Diffractometer facility at IIT Kanpur by the Department of Science and Technology, Government of India is gratefully acknowledged.

Supplementary Material Available: Figures of FAB mass, ^{13}C NMR, and electronic spectra of **1** and **2**, kinetics derivation, tables of crystal data collection and refinement information, thermal parameters of non-hydrogen atoms, calculated hydrogen atom parameters, bond lengths, and bond angles (17 pages); observed and calculated structure factors (54 pages). This material is contained in many libraries on microfiche, immediately follows this article in the microfilm version of the journal, and can be ordered from the ACS; see any current masthead page for ordering information.

(42) (a) Stiefel, E. I.; Newton, W. E.; Watt, G. D.; Hadfield, K. L.; Bulen, W. A. *Adv. Chem. Ser.* **1977**, *162*, 353. (b) Stiefel, E. I.; Gardner, J. K. *J. Less-Common Met.* **1974**, *1*, 521.

(43) Bray, R. C. In *Biological Magnetic Resonance*; Berliner, L. J., Reuben, J., Eds.; Plenum Press: New York, 1980; Vol. 2, p 45.

(44) Pilato, R. S.; Stiefel, E. I. In *Bioinorganic Catalysis*; Reedijk, J., Ed.; Marcel Dekker, Inc: New York, 1993; p 173.